

## Search for Disoriented Chiral Condensates in 158·A GeV Pb+Pb Collisions

Tapan K. Nayak<sup>c</sup> \* *for the WA98 Collaboration*

M.M. Aggarwal<sup>a</sup>, A. Agnihotri<sup>b</sup>, Z. Ahammed<sup>c</sup>, A.L.S. Angelis<sup>d</sup>, V. Antonenko<sup>e</sup>, V. Arefiev<sup>f</sup>, V. Astakhov<sup>f</sup>, V. Avdeitchikov<sup>f</sup>, T.C. Awes<sup>g</sup>, P.V.K.S. Baba<sup>h</sup>, S.K. Badyal<sup>h</sup>, A. Baldine<sup>f</sup>, L. Barabach<sup>f</sup>, C. Barlag<sup>i</sup>, S. Bathe<sup>i</sup>, B. Batiounia<sup>f</sup>, T. Bernier<sup>j</sup>, K.B. Bhalla<sup>b</sup>, V.S. Bhatia<sup>a</sup>, C. Blume<sup>i</sup>, R. Bock<sup>k</sup>, E.-M. Bohne<sup>i</sup>, D. Bucher<sup>i</sup>, A. Buijs<sup>l</sup>, E.-J. Buis<sup>l</sup>, H. Büsching<sup>i</sup>, L. Carlen<sup>m</sup>, V. Chalyshev<sup>f</sup>, S. Chattopadhyay<sup>c</sup>, K.E. Chenawi<sup>m</sup>, R. Cherbatchev<sup>e</sup>, T. Chujo<sup>n</sup>, A. Claussen<sup>i</sup>, A.C. Das<sup>c</sup>, M.P. Decowski<sup>l</sup>, V. Djordjadze<sup>f</sup>, P. Donni<sup>d</sup>, I. Doubovik<sup>e</sup>, M.R. Dutta Majumdar<sup>c</sup>, S. Eliseev<sup>o</sup>, K. Enosawa<sup>n</sup>, H. Feldmann<sup>i</sup>, P. Foka<sup>d</sup>, S. Fokin<sup>e</sup>, V. Frolov<sup>f</sup>, M.S. Ganti<sup>c</sup>, S. Garpman<sup>m</sup>, O. Gavrishchuk<sup>f</sup>, F.J.M. Geurts<sup>l</sup>, T.K. Ghosh<sup>p</sup>, R. Glasow<sup>i</sup>, S.K. Gupta<sup>b</sup>, B. Guskov<sup>f</sup>, H.A. Gustafsson<sup>m</sup>, H.H. Gutbrod<sup>j</sup>, R. Higuchi<sup>n</sup>, I. Hrivnacova<sup>o</sup>, M. Ippolitov<sup>e</sup>, H. Kalechofsky<sup>d</sup>, R. Kamermans<sup>l</sup>, K.-H. Kampert<sup>i</sup>, K. Karadjev<sup>e</sup>, K. Karpio<sup>q</sup>, S. Kato<sup>n</sup>, S. Kees<sup>i</sup>, H. Kim<sup>g</sup>, B.W. Kolb<sup>k</sup>, I. Kosarev<sup>f</sup>, I. Koutcheryaev<sup>e</sup>, A. Kugler<sup>o</sup>, P. Kulinich<sup>r</sup>, V. Kumar<sup>b</sup>, M. Kurata<sup>n</sup>, K. Kurita<sup>n</sup>, N. Kuzmin<sup>f</sup>, I. Langbein<sup>k</sup>, A. Lebedev<sup>e</sup>, Y.Y. Lee<sup>k</sup>, H. Löhner<sup>p</sup>, D.P. Mahapatra<sup>s</sup>, V. Manko<sup>e</sup>, M. Martin<sup>d</sup>, A. Maximov<sup>f</sup>, R. Mehdiyev<sup>f</sup>, G. Mgebrichvili<sup>e</sup>, Y. Miake<sup>n</sup>, D. Mikhalev<sup>f</sup>, G.C. Mishra<sup>s</sup>, Y. Miyamoto<sup>n</sup>, B. Mohanty<sup>s</sup>, D. Morrison<sup>t</sup>, D.S. Mukhopadhyay<sup>c</sup>, V. Myalkovski<sup>f</sup>, H. Naef<sup>d</sup>, B.K. Nandi<sup>s</sup>, S.K. Nayak<sup>j</sup>, T.K. Nayak<sup>c</sup>, S. Neumaier<sup>k</sup>, A. Nianine<sup>e</sup>, V. Nikitine<sup>f</sup>, S. Nikolaev<sup>e</sup>, S. Nishimura<sup>n</sup>, P. Nomokov<sup>f</sup>, J. Nystrand<sup>m</sup>, F.E. Obenshain<sup>t</sup>, A. Oskarsson<sup>m</sup>, I. Otterlund<sup>m</sup>, M. Pachr<sup>o</sup>, A. Parfenov<sup>f</sup>, S. Pavliouk<sup>f</sup>, T. Peitzmann<sup>i</sup>, V. Petracek<sup>o</sup>, F. Plasil<sup>g</sup>, M.L. Purschke<sup>k</sup>, B. Raeven<sup>l</sup>, J. Rak<sup>o</sup>, S. Raniwala<sup>b</sup>, V.S. Ramamurthy<sup>s</sup>, N.K. Rao<sup>h</sup>, F. Retiere<sup>j</sup>, K. Reygers<sup>i</sup>, G. Roland<sup>r</sup>, L. Rosselet<sup>d</sup>, I. Roufanov<sup>f</sup>, J.M. Rubio<sup>d</sup>, S.S. Sambyal<sup>h</sup>, R. Santo<sup>i</sup>, S. Sato<sup>n</sup>, H. Schlagheck<sup>i</sup>, H.-R. Schmidt<sup>k</sup>, G. Shabratova<sup>f</sup>, I. Sibiriak<sup>e</sup>, T. Siemiarczuk<sup>q</sup>, B.C. Sinha<sup>c</sup>, N. Slavine<sup>f</sup>, K. Söderström<sup>m</sup>, N. Solomey<sup>d</sup>, S.P. Sørensen<sup>t</sup>, P. Stankus<sup>g</sup>, G. Stefanek<sup>q</sup>, P. Steinberg<sup>r</sup>, E. Stenlund<sup>m</sup>, D. Stüken<sup>i</sup>, M. Sumbera<sup>o</sup>, T. Svensson<sup>m</sup>, M.D. Trivedi<sup>c</sup>, A. Tsvetkov<sup>e</sup>, C. Twenhöfel<sup>l</sup>, L. Tykarski<sup>q</sup>, J. Urbahn<sup>k</sup>, N.v. Eijndhoven<sup>l</sup>, W.H.v. Heeringen<sup>l</sup>, G.J.v. Nieuwenhuizen<sup>r</sup>, A. Vinogradov<sup>e</sup>, Y.P. Viyogi<sup>c</sup>, A. Vodopianov<sup>f</sup>, S. Vörös<sup>d</sup>, M.A. Vos<sup>l</sup>, B. Wyslouch<sup>r</sup>, K. Yagi<sup>n</sup>, Y. Yokota<sup>n</sup>, and G.R. Young<sup>g</sup>

<sup>a</sup>Univ. of Panjab (India) <sup>b</sup>Univ. of Rajasthan (India) <sup>c</sup>VECC, Calcutta (India) <sup>d</sup>Univ. of Geneva (Switzerland) <sup>e</sup>Kurchatov (Russia) <sup>f</sup>JINR, Dubna (Russia) <sup>g</sup>ORNL, Oak Ridge (USA) <sup>h</sup>Univ. of Jammu (India) <sup>i</sup>Univ. of Münster (Germany) <sup>j</sup>SUBATECH, Nantes (France) <sup>k</sup>GSI, Darmstadt (Germany) <sup>l</sup>NIKHEF, Utrecht (The Netherlands) <sup>m</sup>Univ. of Lund (Sweden) <sup>n</sup>Univ. of Tsukuba (Japan) <sup>o</sup>NPI, Rez (Czech Rep.) <sup>p</sup>KVI, Groningen (The Netherlands) <sup>q</sup>INS, Warsaw (Poland) <sup>r</sup>MIT, Cambridge (USA) <sup>s</sup>IOP, Bhubaneswar (India) <sup>t</sup>Univ. of Tennessee (USA)

The formation of Disoriented Chiral Condensates (DCC) [1] in high energy heavy-ion collisions is associated with large event-by-event fluctuation in the ratio of neutral to charged pions. The probability distribution of neutral pion fraction,  $f$ , in a DCC domain

---

\*email : nayak@veccal.ernet.in

has been shown [2] to follow the relation:

$$P(f) = \frac{1}{2\sqrt{f}} \quad \text{where} \quad f = N_{\pi^0}/N_{\pi} \quad (1)$$

which is quite different from that of the normal pion production mechanism. The detection and study of DCC is expected to provide valuable information about the chiral phase transition and vacuum structure of strong interactions.

Theoretical predictions suggest that the isospin fluctuations caused by DCC would produce clusters of coherent pions in phase space forming domains localized in phase space. However, experimental studies [3] carried out so far have been restricted to global fluctuation in the number of charged particles and photons. Here we present first experimental results to search for localized domains of DCC based on event-by-event fluctuation in the relative number of charged particles and photons detected within the acceptance of the WA98 experiment.

In the WA98 experiment, the main emphasis has been on high precision, simultaneous detection of both hadrons and photons. Charged particle hits ( $N_{\text{ch}}$ ) were counted using a circular Silicon Pad Multiplicity Detector (SPMD) [3] located 32.8 cm downstream of the target with a coverage of  $2.35 < \eta < 3.75$ . Photon multiplicities ( $N_{\gamma\text{-like}}$ ) were measured by the preshower Photon Multiplicity Detector (PMD) [4] placed at 21.5 meters downstream of the target covering an  $\eta$  range of  $2.9 - 4.2$ . It consisted of an array of plastic scintillator pads, arranged inside 28 box modules, placed behind  $3X_0$  thick lead converter plates. A total of 66K central events corresponding to top 5% of the minimum bias cross section, determined from the total transverse energy measured by the midrapidity calorimeter (MIRAC), were analyzed. Common coverage of PMD and SPMD was considered.

Physics analysis with the cleaned data was performed by comparing with mixed and simulated events. Mixed events were constructed from data combining hits from PMD and SPMD chosen randomly from different events taking care of the two track resolutions while maintaining the correlation between  $N_{\gamma\text{-like}}$  and  $N_{\text{ch}}$ , event-wise, as in the data.

Simulated events were generated using VENUS 4.12 event generator with default parameters. The output was then processed through a detector simulation package in the GEANT 3.21 framework. This incorporates the full WA98 experimental setup. The effect of Landau fluctuations in the energy loss of charged particles in silicon [3] was included in the SPMD simulation. For PMD simulation the GEANT results in terms of energy deposition in pads were converted to the pad ADC values taking into account the detector and readout effects. At this stage the simulated data (henceforth referred to as VENUS) and experimental data were ready to be processed with common analysis tools to study specific physics issues.

### $N_{\gamma}$ and $N_{\text{ch}}$ CORRELATION

The correlation between  $N_{\gamma\text{-like}}$  and  $N_{\text{ch}}$  has been studied in smaller  $\phi$ -segments by dividing the  $\phi$ -space into 2, 4, 8 and 16 bins using the method described in Ref. [3]. The correlation plots of  $N_{\gamma\text{-like}}$  and  $N_{\text{ch}}$  have been constructed for each  $\phi$  bin. A common correlation axis ( $Z$ ) has been obtained by fitting the above distributions with a second order polynomial. The closest distance ( $D_Z$ ) of the data points to the correlation axis has been calculated numerically with the convention that  $D_Z$  is positive for points below

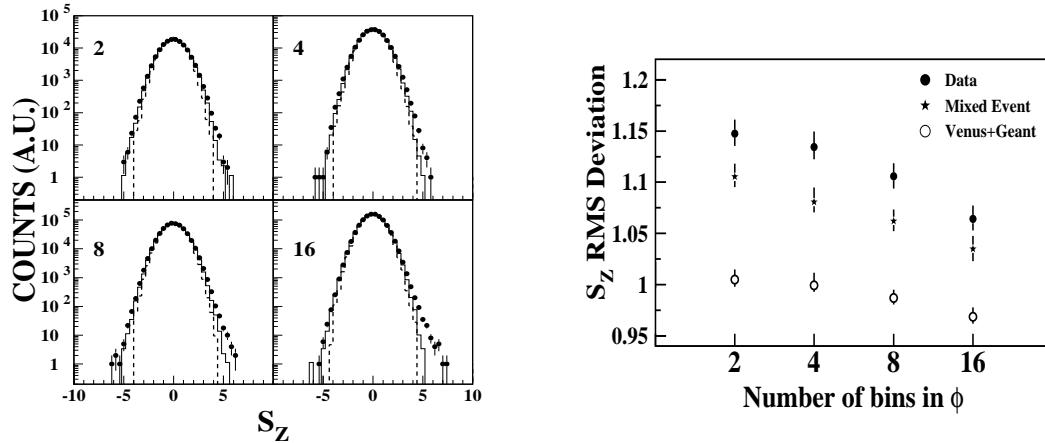


Figure 1. (a)  $S_Z$  distributions for 2,4,8 and 16 divisions in  $\phi$  angle. Solid circles are for data, solid histograms are for mixed events and dashed histograms are for simulation. (b) Corresponding root mean square (rms) deviations. The bars represent systematic errors.

the Z-axis. The distribution of  $D_Z$  represents the relative fluctuations of  $N_{\gamma-like}$  and  $N_{ch}$  from the correlation axis at any given  $\phi$  bin. In order to compare these fluctuations at different scales in the same level, we work with a scaled variable,  $S_Z = D_Z/\sigma(D_Z)$ , where  $\sigma(D_Z)$  corresponds to VENUS events.

The  $S_Z$  distributions are shown in the left panel of Figure 1. The corresponding rms deviations for different  $\phi$  bins are shown in the right of panel of figure 1. The presence of events with DCC domains of a particular size would show up as deviations from general correlation line at the proper bin. This would result in a broader distribution of  $S_Z$  compared to those for generic events at that particular division. From figure 1(b) we also observe that the rms deviations of data differ significantly from those of mixed events when the number of bins in  $\phi$  is 8 or less. This indicates the presence of non-statistical fluctuations in  $N_{\gamma-like}$  and  $N_{ch}$  for bin sizes  $\geq 45^\circ$ .

### DISCRETE WAVELET TECHNIQUE

The novel and powerful method of discrete wavelet transformation (DWT) has also been used for the analysis of the data. Simulation studies by Huang et. al. [5] show that the DWT analysis could be a powerful technique for the search of localized DCC. For the present DWT analysis the azimuthal space of the PMD and the SPMD were divided into small bins in  $\phi$ , the number of bins in a given scale  $j$  being  $2^j$ . The input to the DWT analysis is a spectrum of the sample function at the smallest bin in  $\phi$  corresponding to the highest resolution scale,  $j_{max} = 5$ . Our sample function was chosen to be of the form

$$f' = \frac{N_{\gamma-like}}{N_{\gamma-like} + N_{ch}} \quad (2)$$

The output of the DWT consists of a set of wavelet or father function coefficients (FFCs) at each scale, from  $j = 1, \dots, (j_{max} - 1)$ .

The distribution of FFCs for a generic distribution of particles is gaussian in nature [5–7]. However, the presence of DCC-like fluctuation makes the distribution non-gaussian, with a larger rms deviation of the FFC distribution. Comparing the rms deviations of

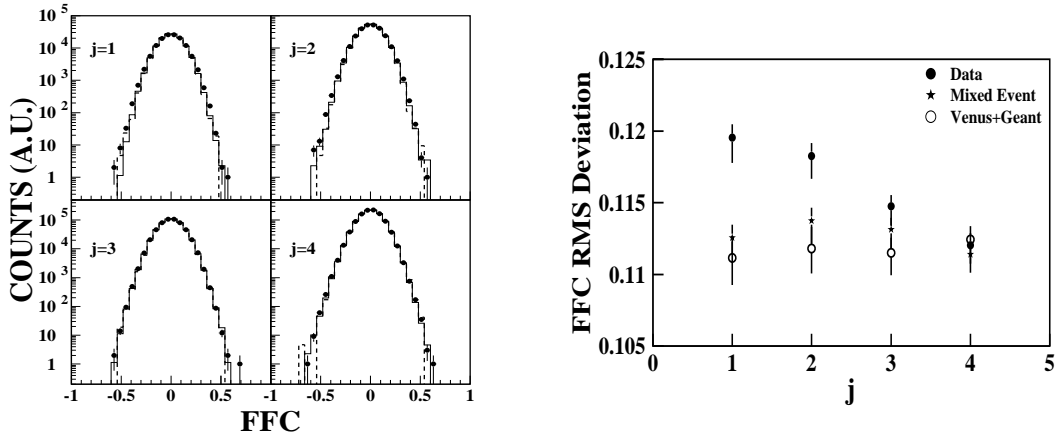


Figure 2. (a) FFC distributions at  $j = 1 - 4$ . Solid circles are for data, solid histograms are for mixed events and dashed histograms are for simulation. (b) Corresponding root mean square (rms) deviations at scales  $j = 1-4$ . The bars represent systematic errors.

the FFC distribution of data, mixed and simulated events one can get an idea about the localized fluctuations in the distributions of  $N_{\gamma-like}$  and  $N_{ch}$  in the azimuthal space.

Figure 2(a) shows the FFC distributions at scales  $j = 1-4$  for data, mixed events and VENUS. The corresponding rms deviations,  $\xi$ , are shown in figure 2(b). We observe that the rms deviations of data, mixed and VENUS events match with each other at scales  $j = 3$  and 4. For scales  $j = 1$  and 2, the rms deviations of VENUS and mixed events are close to each other whereas there is a clear difference of these values from those of the data. In the DWT analysis, the information about the degree of fluctuation at a scale  $j$  is obtained from FFC distribution at scale  $j + 1$ . One can thus deduce that the differences seen at  $j = 2$  and 1 are due to the fluctuations in  $N_{\gamma-like}$  and  $N_{ch}$  at scale  $j = 3$ , i.e. around  $45^\circ$  in  $\Delta\phi$ .

A detailed analysis of the  $\eta - \phi$  phase space distribution of charged particles and photons have been carried out using two independent methods. Both of these indicate the presence of nonstatistical fluctuations in localized regions in terms of photon and charged particle multiplicities. This could have contributions from many different physics effects. Attempts are being made to explain this assuming the fluctuations to be solely due to the presence of localized domains of DCC.

## REFERENCES

1. K. Rajagopal, in *Quark-Gluon Plasma 2* (ed: R. Hwa) World Scientific, 1995.
2. A.A. Anselm, M.G. Ryskin, Phys. Lett. **B266** (1991) 482.
3. M.M. Aggarwal et al., (WA98 Collaboration), Phys. Lett. **B420** (1998) 169.
4. M.M. Aggarwal et al., (WA98 Collaboration), Phys. Lett. **B458** (1999) 422.
5. Zheng Huang, I. Sarcevic, R. Thews and X-N Wang, Phys. Rev. **D54** (1996) 750.
6. B.K. Nandi, G.C. Mishra, B. Mohanty, D.P. Mahapatra and T.K. Nayak, Phys. Lett. **B449** (1999) 109.
7. B.K. Nandi, T.K. Nayak, B. Mohanty, D.P. Mahapatra and Y.P. Viyogi, Phys. Lett., in press (nucl-ex/9903005).